Changes in motor synergies for tracking movement and responses to perturbations depend on task-irrelevant dimension constraints

著者（英）	Shunta Togo, Takahiro Kagawa, Yoji Uno
journal or publication title	Human Movement Science
volume	46
page range	104-116
year	2016-04
URL	http://id.nii.ac.jp/1438/00008857/

doi: 10.1016/j.humov.2015.12.010

Changes in motor synergies for tracking movement and responses to perturbations depend on task-irrelevant dimension constraints

Shunta Togo*, Takahiro Kagawa, and Yoji Uno

Abstract

We investigated the changes in the motor synergies of target-tracking movements of hands and the responses to perturbation when the dimensionalities of target positions were changed. We used uncontrolled manifold (UCM) analyses to quantify the motor synergies. The target was changed from one to two dimensions, and the direction orthogonal to the movement direction was switched from task-irrelevant directions to task-relevant directions. The movement direction was task-relevant in both task conditions. Hence, we evaluated the effects of constraints on the redundant dimensions on movement tracking. Moreover, we could compare the two types of responses to the same directional perturbations in one- and two-dimensional target tasks. In the one-dimensional target task, the perturbation along the movement direction and the orthogonal direction were task-relevant and -irrelevant perturbations, respectively. In the two-dimensional target task, the both perturbations were task-relevant perturbations. The results of the experiments showed that the variabilities of the hand positions in the two-dimensional target-tracking task decreased, but the variances of the

---

*S. Togo[1, 2]

[1]Cognitive Mechanisms Laboratories, Advanced Telecommunications Research Institute International,
2-2-2 Hikaridai, Keihanna Science City, Soraku, Kyoto 619-0288, Japan
[2]Japan Society for the Promotion of Science
Tel: +81-774-95-1029
Fax: +81-774-95-1236
E-mail:togo@atr.jp

T. Kagawa[3] and Y. Uno[3]
[3]Graduate School of Engineering, Nagoya University, Furo-cho, Chikusa-ku, Nagoya 464-8603, Japan

joint angles did not significantly change. For the task-irrelevant perturbations, the variances of the joint angles within the UCM that did not affect hand position (UCM component) increased. For the task-relevant perturbations, the UCM component tended to increase when the available UCM was large. These results suggest that humans discriminate whether the perturbations were task-relevant or -irrelevant and then adjust the responses of the joints by utilizing the available UCM.

Keywords

Redundancy, Uncontrolled manifold analysis, Target tracking, Joint coordination, Synergy

Highlights

- We examined the motor synergy responses to constraints of redundant dimensions.
- Task-relevant hand position variability reduced, but joint variability did not.
- Responses to task-irrelevant perturbations were inhibited.
- Responses to task-relevant perturbations adjusted according to the available UCM.
- Motor synergies adjust according to the available UCM.

1 Introduction

Human multi-joint movements show coordinated flexibility that allows task-irrelevant variability (Latash et al. 2002). Coordinated movements stabilize performance variables that need to be controlled during tasks while allowing the variability of motor elements that do not affect the performance variables or that are redundant in controlling the performance variables. Uncontrolled manifold (UCM) analyses have been proposed for the quantification of coordinated movements (Scholz and Schöner 1999). UCM analyses use a UCM, which is the subspace of motor elements that constructs the same values of a performance variable, and quantitatively evaluate coordinated movements by dividing the variance of the motor elements into components that are parallel and orthogonal to the UCM. Many earlier studies that have applied UCM analyses to examine many kinds of motor tasks have revealed coordinated control strategies of humans (Latash et al. 2007; Latash 2010, 2012; Togo et al. 2012, 2014). UCM analyses divide the variances of motor elements into two components: the UCM component, which does not affect the performance variable, and the orthogonal (ORT) component, which directly affects the performance variable. The ratio of the UCM and ORT components is used to quantify the coordination of motor elements, which is also called the task-dependent motor synergy.

Coordinated strategies that allow task-irrelevant variability and controls task-relevant variability have also been defined as the minimal intervention principle (Todorov and Jordan 2002a, 2002b). The minimal intervention principle states that the human central nervous system (CNS) controls task-relevant variables in order to achieve the task. The findings of some studies have supported the minimal intervention principle based on observations of performance (task-relevant) variables (Liu and Todorov 2007; Valero-Cuevas et al. 2009; Schlerf and Ivry 2011). In the framework of UCM analyses, the minimal intervention principle can be interpreted as control of only the ORT component, while the UCM component is unchanged.

Recently, changes in the UCM component in process of motor learning (Yang et al. 2007; Wu et al. 2012, 2013; Selgrade and Chang 2015) and constraints of motor elements (Togo et al. 2014) have been examined. In our earlier study, we reduced the available degrees of freedom of motor elements with mechanical constraints, and this induced an increase of the UCM component. Moreover, these findings suggested that changes in the available UCM induce changes in motor synergy. In this study, we consider cases in which the available degrees of freedom of motor elements are unchanged, while the dimensionality of the target of the performance variable is changed. In other words, when the available UCM is changed by increasing the dimensionality of the target of the performance variable, how does motor synergy change? Previous studies have examined changes in motor synergy when other physical performance variables are added (Mattos et al. 2011) and when the required accuracy of the performance variable is changed (Tseng et al. 2003, Rosenblatt et al. 2014). However, no studies have examined the effects of changes of the dimensionality of the same physical performance variable. These effects are important to understand in order to determine how changes in the available UCM affect motor synergy and better understand the flexible control mechanisms of human movements. In addition, responses to external perturbations contain important information on the stabilization of multijoint movements. Therefore, in the current study, we evaluated the motor synergies in tracking tasks and their responses to perturbation.

The present study investigated the changes that occurred in motor synergies when the dimensionalities of targets in tracking tasks were changed (Fig. 1a). In the target-tracking task, hand position was the performance variable, and joint angles were the motor elements. The constraint of the dimensionality of the target position of the hand (performance variable) made it possible to separately apply task-relevant and task-irrelevant perturbations. We analyzed the changes in the movement kinematics and the responses to perturbations according to the constraints of the target of the performance variable. We used a motion capture system to record the movement kinematics, and the motor synergy changes were evaluated with the UCM analysis. Moreover, we recorded electromyography (EMG) data to evaluate the neural signals that occurred during the responses to the perturbations. We used an UCM analysis to examine the trial-to-trial variances of joint angles to evaluate motor synergy. We tested the following three hypotheses. First, we examined the effects of performance variable constraints on the variabilities of motor elements. Hence, the first hypothesis was as follows: (a) the task-relevant variabilities of the joints (motor elements) decrease when the dimensionality of the target of the performance variable is constrained. Next, we investigated the changes in the motor synergies that occur to track the target according to the constraints of the task-irrelevant dimensions. The second hypothesis was as follows: (b) the responses to task-irrelevant perturbations are inhibited. Finally, we examined the changes that occurred in response to perturbations according to the available UCM. The third hypothesis was as follows: (c) the availability of a large UCM enhances the motor synergies of the responses to task-relevant perturbations. We evaluated the following variables according to these hypotheses and expected the following results. (a) When the target of the performance variable was constrained, the trial-to-trial total variance of the joint angles would decrease in trials without perturbations. (b) The UCM component was calculated by using the mean trajectories of the trials without perturbations. Thus, the UCM component would increase when task-irrelevant perturbations are applied. Finally, (c) the UCM component was calculated by using the mean trajectories of the trials with perturbations along the movement direction. Thus, the UCM component would increase when task-relevant perturbations are applied. Hypothesis (a) is based on the following inference. Constraints on the performance variable change a part of variance within the UCM into the task-relevant variance of the motor elements (variance orthogonal to the UCM). Therefore, the task-relevant variance of joints would be reduced according to the minimal intervention principle. Hypothesis (b) is derived from the inference that responses to task-irrelevant perturbations would be inhibited based on the minimal intervention principle. Hypothesis (c) is derived from the inference that a variety of corrective responses to task-relevant perturbations would be adoptable when the available UCM is large.

2 Materials and methods

2.1 Subjects

Five healthy right-handed males participated in the experiments. Their average age was 23.4 years (range, 22–27), and their average height and weight were 170.6 cm (168–174) and 61.0 kg (53–68), respectively. Our experiments were approved by the Nagoya University Ethical Review Board. The experimental procedure was explained to all of the participants who provided written informed consents.

2.2 Apparatus

We used a three-dimensional position measurement system (Optotrak Certus, Northern Digital Inc., Waterloo, ONT, CAN) to record the kinematics data at 120 Hz. Infrared-ray markers (7-mm diameter) were placed on four anatomical landmarks of the subjects' arms, including the center of gyration of the shoulder, elbow, and wrist and the tip of the index finger (Fig. 1b). The index finger was fixed in an extended position. We used an EMG measurement system (MQ8, Marq-Medical, Farum, Denmark) at 1,000 Hz to record muscle activity that is considered motor commands from the CNS. We recorded the EMGs of eight muscles that are associated with horizontal shoulder flexion (the greater pectoral muscle and anterior deltoid) and extension (trapezius and posterior deltoid), elbow flexion (biceps) and extension (triceps), and wrist flexion (flexor carpi radialis) and extension (extensor carpi radialis longus). Subjects sat on a rigid chair, and a head-mounted display (HMD) (HMZ-T1, Sony Corporation, Tokyo, Japan) was secured to their heads so they could visualize their hand and target hand positions. The refresh rate of the HMD screen was 60 Hz. To apply mechanical perturbations to the hand position, the index finger was connected to the tip of a two-link robot arm (MMSE Units, Man-Machine Synergy Effectors, Inc., Shiga, Japan) (Fig. 1b). A small three-axis load cell (USL06-H5-500N, Tec Gihan Co., Ltd., Kyoto, Japan) was attached to the tip of the robot arm to measure the force acting on the subject's hand. Except for the mechanical perturbation, the interaction force between the robot arm and the subject's hand was canceled by the force feedback control of the robot arm.

2.3 Procedure

The subjects performed target-tracking tasks in the experimental environment shown in Fig. 1b. Their initial arm posture was given as $\theta_{shoulder} = \pi/4$, $\theta_{elbow} = \pi/2$, and $\theta_{wrist} = \pi/6$. To adjust the initial postures accurately in all of the trials, the subjects placed their elbow, wrist, and fingertip in the initial posture with an accuracy of ±2 mm. The information on the initial posture was displayed by the HMD. After the initial posture adjustment phase, a countdown of 3 s was displayed on the HMD. After the countdown, the subjects performed a trial of the target-tracking task. At the end of each trial, they were given feedback on the sum of the tracking error over the whole movement duration of 5 s. The mechanical perturbation that was applied to the subject's hand in the middle of the whole movement duration (from 2.5 to 2.7 s) was generated by the robot arm, which was controlled such that the hand was exposed to an external force of 10 N for 0.2 s in the +*X*- (lateral) or +*Y*- (anterior) directions. During the initial posture adjustment phase, the target-tracking phase after the countdown, and the wait phase after the movement's end, the robot arm was controlled so that the subjects could freely move their hand.

We specified the following two task conditions in which the dimensionality of the target hand position and the perturbation differed (Fig. 1a):

1. One-dimensional target-tracking task: The end position, target hand position, and subject's hand position were specified only for the *X*-direction (Fig. 1c). The *Y*-direction was the task-irrelevant direction in which movement did not affect task achievement. When the mechanical perturbations were applied in each direction, the +*X*- and +*Y*-directional perturbations were the task-relevant and task-irrelevant perturbations, respectively.
2. Two-dimensional target-tracking task: The end position, target hand position, and subject's

hand position were specified for both the *X*- and *Y*-directions (Fig. 1d). The *Y*-direction was the task-relevant direction in which movement affected task achievement. When the mechanical perturbations were applied in each direction, both the +*X*- and +*Y*-directional perturbations were the task-relevant perturbations.

We analyzed the data of the trials in which Y-directional perturbations were applied. In the one-dimensional target-tracking task, the hand movements in the *Y*-direction did not need to be corrected. In contrast, the hand movements in the *Y*-direction had to be corrected in the two-dimensional target-tracking task (Fig. 1a). The *X*-direction was the task-relevant direction in both task conditions, and the *Y*-direction was switched from the task-irrelevant direction to the task-relevant direction by constraints of the target dimension (from one to two). We then compared the responses to the task-relevant and task-irrelevant perturbations across the task conditions.

The subjects performed the one-dimensional target-tracking task first and then the two-dimensional target-tracking task for 50 trials. In the first 10 trials, no perturbation was applied. The remaining 40 trials, which consisted of 20 trials without perturbations, 10 with +*X*-directional perturbations, and 10 with anterior +*Y*-directional perturbations, were randomly sorted. Therefore, the subjects could not predict whether perturbations would be applied. The one-dimensional target of the hand was given in the *X*-direction and calculated according to the minimum jerk criterion with which the start and end velocities and accelerations were zero (Flash and Hogan 1985). The target moved 0.3 m in the left direction in 5 s. The target hand position in the *X*-direction in the two-dimensional target-tracking task as well as the minimum-jerk trajectory in the one-dimensional target-tracking task was given. The target in the *Y*-direction was given as the mean trajectory in the first 10 trials without perturbations in the one-dimensional target-tracking task. The subjects practiced the tracking movements with the robot arm before the experiment began. When they felt fatigued, they were allowed to have short breaks.

2.4 Data analysis

The position data were filtered with a second-order Butterworth low-pass filter with a 10-Hz cutoff frequency. We determined the start and end postures and trajectory of the hand from these position data. The joint angles were calculated from the position data of the arm that were determined in the UCM analysis. The movement duration (5 s) was divided into five phases (one phase consisted of 1 s) in order to calculate the mean values of the hand position and each component variance. The EMG data were full-wave rectified, downsampled to 100 Hz, and filtered with a second-order Butterworth low-pass filter with a 10-Hz cutoff frequency. We evaluated the variations of the EMG waveforms from the onset of the perturbation, and the variations were calculated by subtracting the mean waveforms in the task without perturbations from those with perturbations. We calculated the mean waveforms and standard deviations of all the subjects from the mean EMG data of each subject. All of the EMG data of each subject were normalized according to the maximum EMG value.

2.5 UCM analysis

The motor synergies for tracking movements and responses to mechanical perturbations were quantified with the UCM analysis. The UCM is defined by the null space of the Jacobian $\boldsymbol{J}(\overline{\boldsymbol{\theta}})$ between the hand velocity in the *X*-direction and the joint velocity. The null space is spanned by basis vectors, $\boldsymbol{\varepsilon}_i$, according to $0 = \boldsymbol{J}(\overline{\boldsymbol{\theta}}) \cdot \boldsymbol{\varepsilon}_i$. For the n ($n = 3$) dimensions of the joint angles and d ($d = 1$) dimensions of the hand position, the number of basis vectors of the null space was $n - d$. Therefore, the deviations of the joint angles, which were parallel to the UCM, were given as follows:

$$\boldsymbol{\theta}_{\parallel} = \sum_{i=1}^{n-d} \boldsymbol{\varepsilon}_i^T \cdot (\boldsymbol{\theta} - \overline{\boldsymbol{\theta}}) \cdot \boldsymbol{\varepsilon}_i, \quad (1)$$

where $\bar{\boldsymbol{\theta}}$ is the mean joint angle trajectories. The deviation perpendicular to the UCM was calculated as follows:

$$\boldsymbol{\theta}_{\perp} = (\boldsymbol{\theta} - \bar{\boldsymbol{\theta}}) - \boldsymbol{\theta}_{\parallel}. \tag{2}$$

The UCM component (V_{UCM}) and ORT component (V_{ORT}) were then obtained by normalizing them with the number of dimensions as follows:

$$V_{UCM} = \frac{\boldsymbol{\theta}_{\parallel}^{2}}{n-d},$$

$$V_{ORT} = \frac{\boldsymbol{\theta}_{\perp}^{2}}{d}. \tag{3}$$

In addition, we evaluated the normalized total variance (V_{TOT}) as follows:

$$V_{TOT} = \frac{(n-d)\cdot V_{UCM} + d\cdot V_{ORT}}{n}. \tag{4}$$

Across task conditions, we used the same UCM in the analysis. Thus, we were able to compare the changes that occurred in the motor synergies according to the constraints on the target of the performance variable. Moreover, we used two types of mean trajectories of the joint angles to calculate the Jacobian $\boldsymbol{J}(\bar{\boldsymbol{\theta}})$ and deviation ($\boldsymbol{\theta} - \bar{\boldsymbol{\theta}}$): the mean trajectory of the unperturbed trials and the mean trajectory of the perturbed trials. To evaluate the motor synergy of the tracking movement, we used the mean trajectory of the unperturbed trials. To evaluate the motor synergy of the response to the perturbation, we used two mean trajectories. The mean trajectory of the unperturbed trials was used to quantify the motor synergy for achievement of the task. In contrast, the mean trajectory of the perturbed trials was used to quantify the motor synergy stabilizing response to the perturbation.

2.6 Statistical analysis

In order to analyze the data in the tracking task without perturbation, we compared the standard deviations of the hand position, total variances of the joints, and the UCM and ORT components between the task conditions. We divided the time profiles of these variables by bins (1 bin per 1 s) and considered 1 bin as 1 phase. We performed a two-way repeated measures analysis of variance (ANOVA) to examine the effects of phase (phase 1–5) and task condition (one- and two-dimensional targets) on the kinematic data. For the post hoc test, a paired *t*-test was used to compare the kinematic data between the two task conditions (α = 0.05). In addition, we compared the responses to the *Y*-directional perturbations (UCM component, ORT component, and EMG) and *X*-directional perturbations (UCM component and ORT component) between the task conditions. We divided the time profiles of these variables after onset of the perturbations by bins (1 bin per 0.1 s). A two-way ANOVA was performed to examine the effects of phase (phase 1–15) and task condition (one- and two-dimensional targets). In addition, we performed paired *t*-tests to compare the responses to the perturbations between the two task conditions (α = 0.05).

3 Results

3.1 Movement kinematics

We compared the movement kinematics between the one- and two-dimensional target-tracking tasks. Figs. 2a and 2c show the start and end arm postures in each task of a typical subject. The black solid lines on the right side denote the initial arm postures in all of the trials, and the gray solid and black dashed lines on the left side denote the end arm postures in the trials without perturbation and with *Y*-directional perturbation. In the one-dimensional target-tracking task, the hand position at the movement end was more varied in the task-irrelevant direction (*Y*-direction), even without perturbation. Moreover, the hand position at the movement end shifted to the direction in which the perturbation was given. In the two-dimensional target-tracking task, the variance of the hand position at the movement end was the same as that at the movement start, which indicated that the hand position converged to the target against the perturbation. Figs. 2b and 2d show the hand trajectory in each task of a typical subject. The typical hand trajectories that occurred around the perturbation onset are enlarged and shown on the right side. When the hand was perturbed by the robot arm, it still moved in the -*X*-direction due to inertia after the perturbation onset. Subsequently, the hand was moved to the +*Y*-direction by the robot arm. In the one-dimensional target-tracking task, the hand trajectory deviated to the perturbed direction and reached the end position without corrective movements. However, in the two-dimensional target-tracking task, the perturbed hand position converged to the target hand position after the perturbation.

Fig. 3 shows the standard deviations of the hand trajectories in each task of all of the subjects. These standard deviations were calculated from the trajectories of the unperturbed trials. A two-way ANOVA indicated that the standard deviations of the hand trajectories in the *X*-direction differed significantly between task conditions [$F(1, 40) = 4.55$, $P = 0.039$, Fig. 3c]. In the *Y*-direction, a two-way ANOVA showed a significant task effect [$F(1, 40) = 26.8$, $P = 6.67 \times 10^{-6}$], which indicated that the standard deviations of the hand trajectories in the *Y*-direction were significantly larger in the one-dimensional target-tracking task (Figs. 3b and 3d). These results indicated that the task-irrelevant variability of hand position was allowed during the tracking task.

Fig. 4 shows the component variance in each task of all of the subjects. A two-way ANOVA did not indicate any significant task effects of the variance of each component [Total: $F(1, 40) = 0.12$, $P = 0.73$; UCM: $F(1, 40) = 0.11$, $P = 0.75$; ORT: $F(1, 40) = 0.37$, $P = 0.54$]. These results indicated that constraints on the target of the performance variable did not significantly affect the component variance of the joints. Moreover, the UCM components were greater than the ORT components, which indicated that hand position was controlled in a coordinated manner in both tasks.

3.2 Response to perturbation

The UCM analysis and EMG data for the responses to the perturbations were used to examine the responses to perturbation. First, we analyzed the responses to Y-directional perturbations. Fig. 5 shows the UCM and ORT components that were calculated from the mean trajectories of the unperturbed trials. The UCM component differed significantly between the one- and two-dimensional target-tracking tasks after perturbation [two-way ANOVA, task effect: $F(1, 120) = 102.6$, $P = 8.43 \times 10^{-18}$]. Similarly, the ORT component differed significantly [two-way ANOVA, task effect: $F(1, 120) = 5.11$, $P = 0.026$]. Paired t-tests showed significantly different phases in the UCM component ($P < 0.05$) and no differences in the ORT component. The Y-direction was the task-irrelevant direction for the one-dimensional target. Therefore, the subjects did not have to correct their Y-directional hand movements, and variance from the mean trajectories of the unperturbed trials was allowed. In contrast, the task-relevant variance was immediately corrected for the two-dimensional target. In addition, we evaluated the EMG waveforms of the biceps (elbow flexion) and flexor carpi radialis (wrist flexion), which mainly generate torque against the Y-directional perturbation. The EMG data of the biceps and flexor carpi radialis are shown in Fig. 6. The timings of the EMG peaks were almost the same between the one- and two-dimensional target-tracking tasks, and the peak in the two-dimensional task exceeded that in the one-dimensional tasks. A two-way ANOVA indicated that the EMG waveforms were significantly larger in the two-dimensional target-tracking task than those in the one-dimensional task [task effect: elbow, $F(1, 120) = 33.1$, $P = 6.82 \times 10^{-8}$; wrist, $F(1, 120) = 40.42$, $P = 3.86 \times 10^{-9}$]. These results indicated that the subjects adjusted their responses to the perturbation according to on the task relevance of the perturbation.

Second, the responses to the X-directional perturbations were analyzed. Fig. 7 shows the UCM and ORT components that were calculated from the mean trajectories of the trials with X-directional perturbations. A two-way ANOVA showed significant task effects of the UCM component [$F(1, 120) = 13.9$, $P = 2.98 \times 10^{-4}$] and ORT component [$F(1, 120) = 8.96$, $P = 0.003$]. However, paired t-tests did not indicate any significant differences in any of the phases. The UCM component in the one-dimensional target-tracking task tended to be larger than that in the two-dimensional task. These results weakly indicated that the subjects tended to adopt more flexible responses to the task-relevant perturbations when the available UCM was large.

4 Discussion

The present study investigated the changes that occurred in the motor synergies of tracking task and the responses to perturbation when the target of the performance variable was constrained or, in other words, when the available UCM was reduced. The following three hypotheses were tested: (a) the task-relevant variability of joint angles decreases when the target of the performance variable is constrained; (b) response to task-irrelevant perturbation is inhibited when the target of the performance variable is not constrained; and (c) the availability of a large UCM enhances the motor synergy of the response to task-relevant perturbation. With respect to hypothesis (a), the task-relevant variability of hand position in the workspace was reduced when the target of the performance variable was constrained (Figs. 3b and 3d). However, the variance of the joint angles did not significantly change, and the average value tended to increase rather than decrease (Fig. 4). Therefore, hypothesis (a) was rejected, but the minimal intervention principle was not rejected. Our results suggested that humans do not necessarily reduce the variability of motor elements when he/she reduces the task-relevant variabilities of performance variables in accordance with the minimal intervention principle. For the hypothesis (b), the same Y-directional perturbation induced different responses depending on the task conditions. When a task-irrelevant perturbation was applied in the one-dimensional target-tracking task, the response to the perturbation was inhibited, and the task-irrelevant trial-to-trial variance was allowed and remained (Figs. 2, 5, and 6). However, when a task-relevant perturbation was applied in the two-dimensional target-tracking task, the response to the perturbation was enhanced, and the task-relevant variance was reduced. The above results supported hypothesis (b). With respect to hypothesis (c), the same *X*-directional perturbation that was relevant to task performance was applied to the subject's hand in both task conditions. When the available UCM was large in the one-dimensional target-tracking task, the UCM component of the response to the perturbation tended to be larger than that in the two-dimensional target-tracking task (Fig. 7). Thus, hypothesis (c) was weakly supported. The results of this study suggested that the CNS discriminated whether a perturbation was task-relevant or task-irrelevant, adjusted the response, and utilized the available UCM to flexibly respond to the perturbation.

We tested hypothesis (a) according to the minimal intervention principle. Conventionally, reductions of the variability of motor elements have been assumed to decrease the variability of a performance variable. Fig. 8 illustrates the UCM in the joint space and its relationship to constraints of the target of the performance variable. In the one-dimensional target-tracking task, the UCM was a plane, and we therefore assumed that the trial-to-trial variability of the joints was distributed so that the probability ellipse became a solid circle, as shown in Fig. 8a. In the two-dimensional target-tracking task, the available UCM is represented as the dashed line shown in Fig. 8a. Here, we will discuss the effects of changing the target from one dimension to two dimensions. If the total variance is reduced from $V_{TOT}|_{1d}$ to $V_{TOT}|_{2d}$, as shown in Fig. 8a, the UCM component decreases when the UCM analysis with $UCM|_{1d}$ is applied in both tasks. In earlier studies that used UCM analyses, the UCM and ORT components in a simple task were decreased with practice (Domkin et al.

2002; Yang and Scholz 2005). In earlier studies, the whole trial-to-trial variability of motor elements and the variability of the performance variable were reduced. However, in this study, the UCM component in the trials without perturbations did not change significantly between the two task conditions (Fig. 4e). Rather, the UCM component tended to be larger in the two-dimensional target-tracking task than that in the one-dimensional task at phase 5. The human CNS adopts the strategy of not changing the amount of variability and changing the distribution of variability according to the available UCM, as shown in Fig. 8b. The findings of recent studies involving UCM analyses have suggested that humans adopt a strategy of increasing the UCM component according to the task difficulty (Wu et al. 2012, 2013; Togo et al. 2014). Moreover, Rosenblatt et al. (2014) have reported that, when accurate control of a swing foot, which was one of the performance variables in locomotion, was required, the variability of the swing foot decreased, while the variability of the related joint angles of the lower limbs increased. The results of earlier and present studies suggest that the CNS does not necessarily reduce the variability of motor elements when the error of the performance variable is corrected, and it flexibly utilizes the available UCM to control the performance variable. The observations of the same tendencies in the upper limb movements in the present study and in the lower limb movements in an earlier study suggested that such a flexible strategy is the general strategy for whole body movements.

As shown in Fig. 2, the arm trajectories differed in each task, even though the same *Y*-directional perturbation was applied. When a *Y*-directional perturbation was applied in the one-dimensional target-tracking task, the subject's hand shifted in the perturbed direction and reached the end position without a corrective movement, which shifted the hand position at the end of the movement in the perturbed direction. When a *Y*-directional perturbation was applied in the two-dimensional target-tracking task, the hand moved in the perturbed direction but immediately converged to the target hand trajectory. Moreover, we evaluated the EMG data, as shown in Fig. 6. The subjects showed a significantly larger EMG peak in the two-dimensional target tracking task. The results of the movement kinematics and EMG data described above indicated that the human motor control system discriminates the direction affecting the task achievement and the direction that is allowed to vary in the joint space. With respect to the minimal intervention principle, responses to task-relevant perturbations have recently been reported to be enhanced, while the responses to task-irrelevant perturbations were inhibited (Diedrichsen 2007; Franklin and Wolpert 2008). Moreover, such response modulations can be achieved by only using somatosensory information without visual information (Dimitriou et al. 2012). In this study, the task achievement was determined with only visual information. The results of the UCM analysis therefore suggested that the human somatosensory feedback control system utilized the information corresponding to the UCM that was constructed with visual information.

With respect to hypothesis (c), the UCM component that was calculated from the mean trajectories of the perturbed trials tended to increase in the one-dimensional target-tracking task (Fig. 7). In both task conditions, the responses to the X-directional perturbations were task-relevant corrective responses. The available UCM was larger in the one-dimensional target-tracking task compared with the two-dimensional task. These results indicated that the task-relevant corrective responses were affected by the available UCM. Because the UCM component was large, especially about 1 s after the perturbation was applied, the corrective response was flexibly adjusted with visual information. These results suggested that the larger the UCM was, the more flexible the strategy was for the corrective response. Some earlier studies have analyzed the kinematics of responses to perturbations with UCM analyses (Scholz et al. 2007; Mattos et al. 2011). Mattos et al. (2011) have reported that humans coordinate whole body joints in order to stabilize the position of the center of mass in response to perturbations, which indicated that the corrective responses to the perturbations were not predetermined and unique, but quite flexible. Moreover, the results of our study provided the additional suggestion that such a flexible corrective response was affected by the available UCM.

The results of our study suggested a somatosensory feedback loop with a mechanism that discriminates whether the variability affected task achievement. Two strategies can be applied to achieve the control mechanism described above. The first is the feedforward adjustment of hand stiffness. The CNS can adjust joint stiffness to an appropriate value depending on task conditions (Gribble et al. 2003; Osu et al. 2004, 2009; Koike et al. 2006). Isometric conditions have been reported to easily control the size of the hand stiffness ellipsoid, while control of its direction is difficult (Gomi and Osu 1998; Perreault et al. 2002; Darainy et al. 2004). During movement, the CNS can appropriately adjust the direction of the hand stiffness ellipsoid according to the dynamics of the environment (Franklin et al. 2007). In this study, the CNS adjusted the value of the joint stiffness in parallel with the anterior-posterior direction according to the one- and two-dimensional target-tracking tasks. If appropriate impedance parameters are determined before the task, the subjects could respond to the perturbation earlier than when visual feedback is used. In the feedforward strategy, information corresponding to the UCM is utilized to determine appropriate stiffness. The second strategy is corticospinal feedback. The human motor control model in computational neuroscience assumes that the brain solves the inverse problem of transformation from information on the workspace (e.g., hand position) to information on the joint space (e.g., joint angle) (Flash and Sejnowski 2001; Schaal and Schweighofer 2005; Campos and Calado 2009). Physiological studies have reported that the activities of neurons in the motor cortex correlate both with information for workspace (Georgopoulos et al. 1984; Flament and Hore 1988; Moran and Schwartz 1999) and joint space (Thach 1978; Fetz and Cheney 1980; Reina et al. 2001). The UCM in arm movement is the joint space information that is produced from workspace information. For the mechanical perturbations examined in this study, the CNS judged whether the perturbation was task-relevant or task-irrelevant through somatosensory information and the UCM and changed the response accordingly. The feedforward strategy and/or feedback strategy utilizing the UCM was applied to achieve the task.

When the hand was perturbed in the task-irrelevant direction, it shifted to the perturbed direction, and the movement in the redundant direction was then stopped. The end position was reached without corrective movements (Figs. 2a and b). Movements in redundant dimensions have been called self-motion, which is an area of research in the field of robotics (Burdick 1989). By controlling a robot arm without joint viscosity, self-motion is a joint movement that is continued while movement of an end effector is terminated. In many robotics studies, self-motion is suppressed through the virtual viscosity of each joint (e.g., Arimoto et al. 2005). In human movements, Martin et al. (2009) have reported that at least 30% of human joint velocity is self-motion in point-to-point reaching movements. Whether self-motion is a result of neural control or a passive brake due to the viscous properties of muscles is an interesting question. Fig. 6 shows that a small peak in the EMG waveform opposing the perturbation appeared even in the one-dimensional target-tracking task. These results that are based on the musculoskeletal dynamics of the human arm reflect corrective movements in response to task-relevant variability. The stretch reflex of the muscle was also affected by movements in the redundant direction. Therefore, the brakes from the passive viscous properties of muscles and controls that include reflex mechanisms stop self-motion. Important issues to examine in the future are the estimation of the viscous properties of muscles and the control mechanisms of self-motion.

5. Conclusion

In this study, we examined the changes that occur in motor synergies when the dimensionality of the target of a performance variable was changed in a tracking task. The tracking target was changed from one to two dimensions, and the direction orthogonal to the movement direction was switched from a task-irrelevant direction to a task-relevant direction. The perturbations in movement direction were task-relevant directions in both task conditions, while those in the orthogonal direction were in task-irrelevant and task-relevant direction in the one- and two-dimensional task conditions, respectively. The subjects performed the target-tracking tasks, and their movement kinematics and EMG data were measured. UCM analyses were used to quantify the motor synergies for the tracking task and the responses to perturbations. The following three hypotheses were tested, and the following results were obtained: (a) When the target of the performance variable was constrained, the task-relevant variance of the joint angles decreased. As a result, the variability of hand position decreased, but the variance of the joint angles did not change significantly, which resulted in a rejection of the hypothesis. (b) Responses to task-irrelevant perturbations were inhibited when the target of the performance variable was not constrained. The results showed that the trial-to-trial variance within the UCM that was calculated from the mean trajectory of the unperturbed trials increased, and the EMG peak decreased in one-dimensional target-tracking tasks, which supported the hypothesis. (c) The availability of a large UCM enhanced the motor synergy of responses to task-relevant perturbations. The results indicated that the UCM component that was calculated from the mean trajectory of the perturbed trials tended to increase when the available UCM was large, which weakly supported the hypothesis. These results suggested that the human CNS does not necessarily reduce the variability of motor elements so as to reduce the variability of the performance variable. Moreover, we concluded that the CNS discriminated whether the perturbation was task-relevant or task-irrelevant, adjusted the response, and utilized the available UCM to produce a flexible response.

Acknowledgments

This research was supported by a Japan Society for the Promotion of Science (JSPS) Grant-in-Aid for JSPS Fellows 267576 and Grants-in-Aid for Scientific Research (B) 26289129 and 26280101.

References

Arimoto S, Hashiguchi H, Sekimoto M, Ozawa R (2005) Generation of natural motions for redundant multi-joint systems: A differential-geometric approach based upon the principle of least actions. J Robotic Syst 22:583-605

Burdick JW (1989) On the inverse kinematics of redundant manipulators: Characterization of the self-motion manifolds. In: Proceedings of the IEEE International Conference on Robotics and Automation, pp. 264-270

Campos FMMO, Calado JMF (2009) Approaches to human arm movement control–a review. Annu Rev Control 33:69-77

Darainy M, Malfait N, Gribble PL, Towhidkhah F, Ostry DJ (2004) Learning to control arm stiffness under static conditions. J Neurophysiol 92:3344-3350

Diedrichsen J (2007) Optimal task-dependent changes of bimanual feedback control and adaptation. Curr Biol 17:1675-1679

Dimitriou M, Franklin DW, Wolpert DM (2012) Task-dependent coordination of rapid bimanual motor responses. J Neurophysiol 107:890-901

Domkin D, Laczko J, Jaric S, Johansson H, Latash ML (2002) Structure of joint variability in bimanual pointing tasks. Exp Brain Res 143:11-23

Fetz EE, Cheney PD (1980) Postspike facilitation of forelimb muscle activity by primate corticomotoneuronal cells. J Neurophysiol 44:751-772

Flament D, Hore J (1988) Relations of motor cortex neural discharge to kinematics of passive and active elbow movements in the monkey. J Neurophysiol 60:1268-1284

Flash T, Hogan N (1985) The coordination of arm movements: an experimentally confirmed mathematical model. J Neurosci 5:1688-1703

Flash T, Sejnowski TJ (2001) Computational approaches to motor control. Curr Opin Neurobiol 11:655-662

Franklin DW, Liaw G, Milner TE, Osu R, Burdet E, Kawato M (2007) Endpoint stiffness of the arm is directionally tuned to instability in the environment. J Neurosci 27:7705-7716

Franklin DW, Wolpert DM (2008) Specificity of reflex adaptation for task-relevant variability. J Neurosci 28:14165-14175

Georgopoulos AP, Caminiti R, Kalaska JF (1984) Static spatial effects in motor cortex and area 5: Quantitative relations in a two- dimensional space. Exp Brain Res 54:446-454

Gomi H, Osu R (1998) Task-dependent viscoelasticity of human multijoint arm and its spatial characteristics for interaction with environments. J Neurosci 18:8965-8978

Gribble PL, Mullin LI, Cothros N, Mattar A (2003) Role of cocontraction in arm movement accuracy. J Neurophysiol 89:2396-2405

Koike Y, Kim J, Duk S (2006) Role of stiffness in weight perception. Jpn Psychol Res 48:174-187

Latash ML (2010) Stages in learning motor synergies: A view based on the equilibrium-point hypothesis. Hum Mov Sci 29:642-654

Latash ML (2012) Movements that are both variable and optimal. J Hum Kinet 34:5-13

Latash ML, Scholz JP, Schöner G (2002) Motor control strategies revealed in the structure of motor variability. Exerc Sport Sci Rev 30:26-31

Latash ML, Scholz JP, Schöner G (2007) Toward a new theory of motor synergies. Motor Control 11:276-308

Liu D, Todorov E (2007) Evidence for the flexible sensorimotor strategies predicted by optimal feedback control. J Neurosci 27:9354-9368

Martin V, Scholz JP, Schöner G (2009) Redundancy, self-motion, and motor control. Neural Comput 21:1371-1414

Mattos DJ, Latash ML, Park E, Kuhl J, Scholz JP (2011) Unpredictable elbow joint perturbation during reaching results in multijoint motor equivalence. J Neurophysiol 106:1424-1436

Moran DW, Schwartz AB (1999) Motor cortical representation of speed and direction during reaching. J Neurophysiol 82:2676-2692

Osu R, Morishige K, Miyamoto H, Kawato M (2009) Feedforward impedance control efficiently reduce motor variability. Neurosci Res 65:6-10

Osu R, Kamimura N, Iwasaki H, Nakano E, Harris CM, Wada Y, Kawato M (2004) Optimal impedance control for task achievement in the presence of signal-dependent noise. J Neurophysiol 92:1199-1215

Perreault EJ, Kirsch RF, Crago PE (2002) Voluntary control of static endpoint stiffness during force regulation tasks. J Neurophysiol 87:2808-2816

Reina GA, Moran DW, Schwartz AB (2001) On the relationship between joint angular velocity and motor cortical discharge during reaching. J Neurophysiol 85:2576-2589

Rosenblatt NJ, Hurt CP, Latash ML, Grabiner MD (2014) An apparent contradiction: increasing variability to achieve greater precision? Exp Brain Res 232:403-413

Schaal S, Schweighofer N (2005) Computational motor control in humans and robots. Curr Opin Neurobiol 15:675-682

Schlerf JE, Ivry RB (2011) Task goals influence online corrections and adaptation of reaching movements. J Neurophysiol 106:2622-2631

Scholz JP, Schöner G, Hsu WL, Jeka JJ, Horak F, Martin V (2007) Motor equivalent control of the center of mass in response to support surface perturbations. Exp Brain Res 180:163-179

Scholz JP, Schöner G (1999) The uncontrolled manifold concept: identifying control variables for a functional task. Exp Brain Res 126:289-306

Selgrade BP, Chang YH (2015) Locomotor control of limb force switches from minimal intervention principle in early adaptation to noise reduction in late adaptation. J Neurophysiol 113:1451-1461

Thach WT (1978) Correlation of neural discharge with pattern and force of muscular activity, joint position, and direction of intended next movement in motor cortex and cerebellum. J Neurophysiol 41:654-676

Todorov E, Jordan MI (2002a). A Minimal Intervention Principle for Coordinated Movement, In: Advances in Neural Information Processing Systems 15. Becker S, Thrun S, Obermayer K (eds.), MIT Press, Cambridge, MA, pp. 27-34

Todorov E, Jordan MI (2002b) Optimal feedback control as a theory of motor coordination. Nat Neurosci 5:1226-1235

Togo S, Kagawa T, Uno Y (2012) Motor synergies for dampening hand vibration during human walking. Exp Brain Res 216:81-90

Togo S, Kagawa T, Uno Y (2014) Change of a motor synergy for dampening hand vibration depending on a task difficulty. Exp Brain Res 232:3101-3109

Tseng YW, Scholz JP, Schöner G, Hotchkiss L (2003) Effect of accuracy constraint on joint coordination during pointing movements. Exp Brain Res 149:276-288

Valero-Cuevas FJ, Venkadesan M, Todorov E (2009) Structured variability of muscle activations supports the minimal intervention principle of motor control. J Neurophysiol 102:59-68

Wu YH, Pazin N, Zatsiorsky VM, Latash ML (2012) Practicing elements vs. practicing coordination: Changes in the structure of variance. J Mot Behav 44:471-478

Wu YH, Pazin N, Zatsiorsky VM, Latash ML (2013) Improving finger coordination in young and elderly persons. Exp Brain Res 226:273-283

Yang JF, Scholz JP (2005) Learning a throwing task is associated with differential changes in the use of motor abundance. Exp Brain Res 163:137-158

Yang JF, Scholz JP, Latash ML (2007) The role of kinematic redundancy in adaptation of reaching. Exp Brain Res 176:54-69

Figures

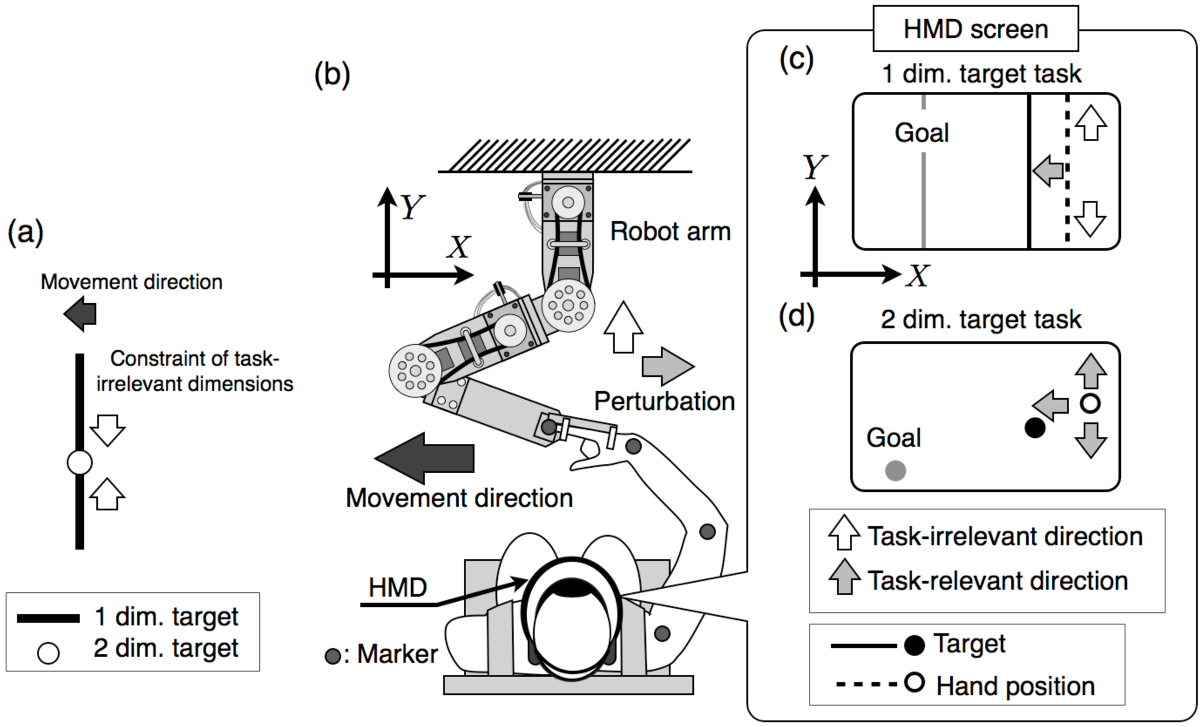

Fig. 1 Concept of one- and two-dimensional target-tracking tasks and schematic of measurement experiment. (a) The one- and two-dimensional targets are given by the line and point, respectively. The task-irrelevant direction of one-dimensional target is constrained by the two-dimensional target. (b) Schematic of the measurement experimental setup. The subjects performed one- and two-dimensional target-tracking tasks while sitting on a chair and wearing a seatbelt. The hand of the robot arm is connected to the subject's hand, and it applies mechanical perturbation. A head-mounted display (HMD) is secured to the head, and position measurement markers are placed on arm segments. The one- and two-dimensional hand position of the subject and target are shown on the HMD screen. (c) HMD screen for the one-dimensional target-tracking task in which the *Y*-direction is the task-irrelevant direction. (d) The HMD screen for the two-dimensional target-tracking task in which the *Y*-direction is the task-relevant direction.

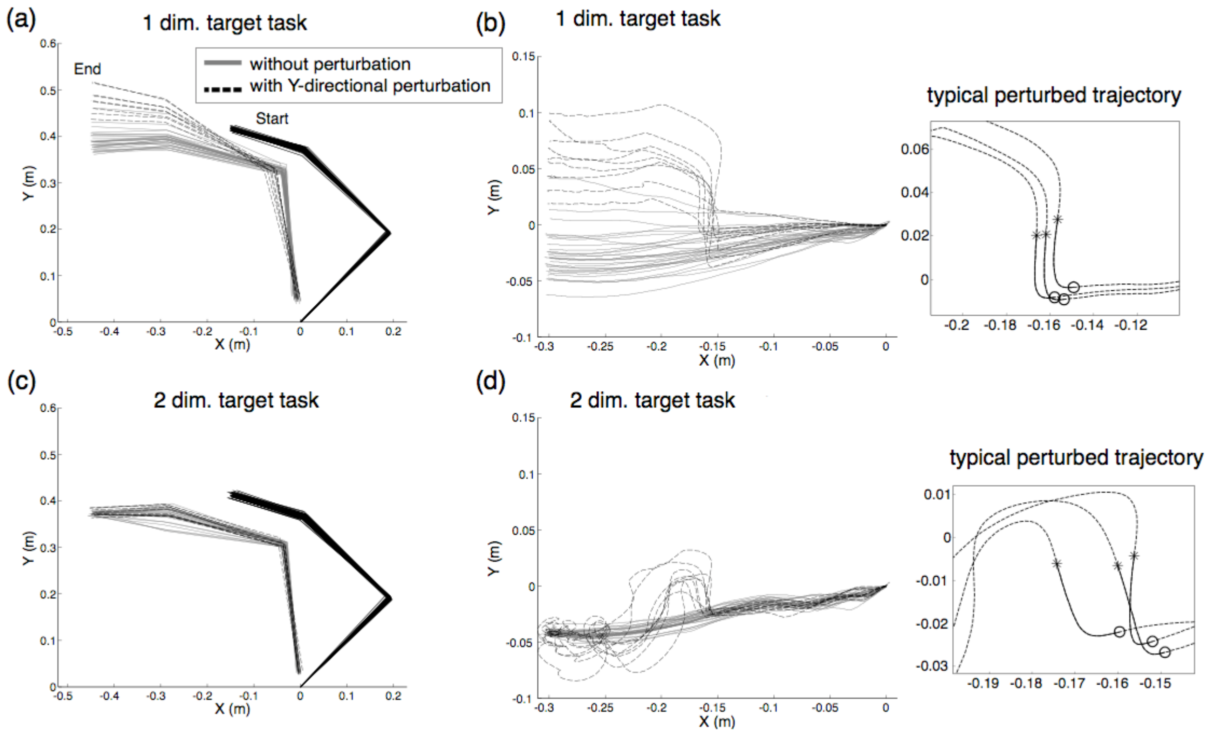

Fig. 2 Kinematics of the arm movements. The figures on the left show the arm postures at the start and end of all of the trials of the one-dimensional target-tracking task (a) and two-dimensional target tracking task (c) of a typical subject. The horizontal and vertical axes denote the medial-lateral and anterior-posterior directions. The black solid lines on the right side denote the initial postures in all of the trials, and the gray solid and black dashed lines on the left side denote the end postures in the trials without perturbation and with *Y*-directional perturbation. The figures on the right show the hand trajectories in all of the trials of the one-dimensional target-tracking task (b) and two-dimensional target-tracking task (d) of a typical subject. The gray solid lines and black dashed lines denote hand trajectories in trials without perturbation and with *Y*-directional perturbations. The circles and asterisks indicate the start and end of the perturbation.

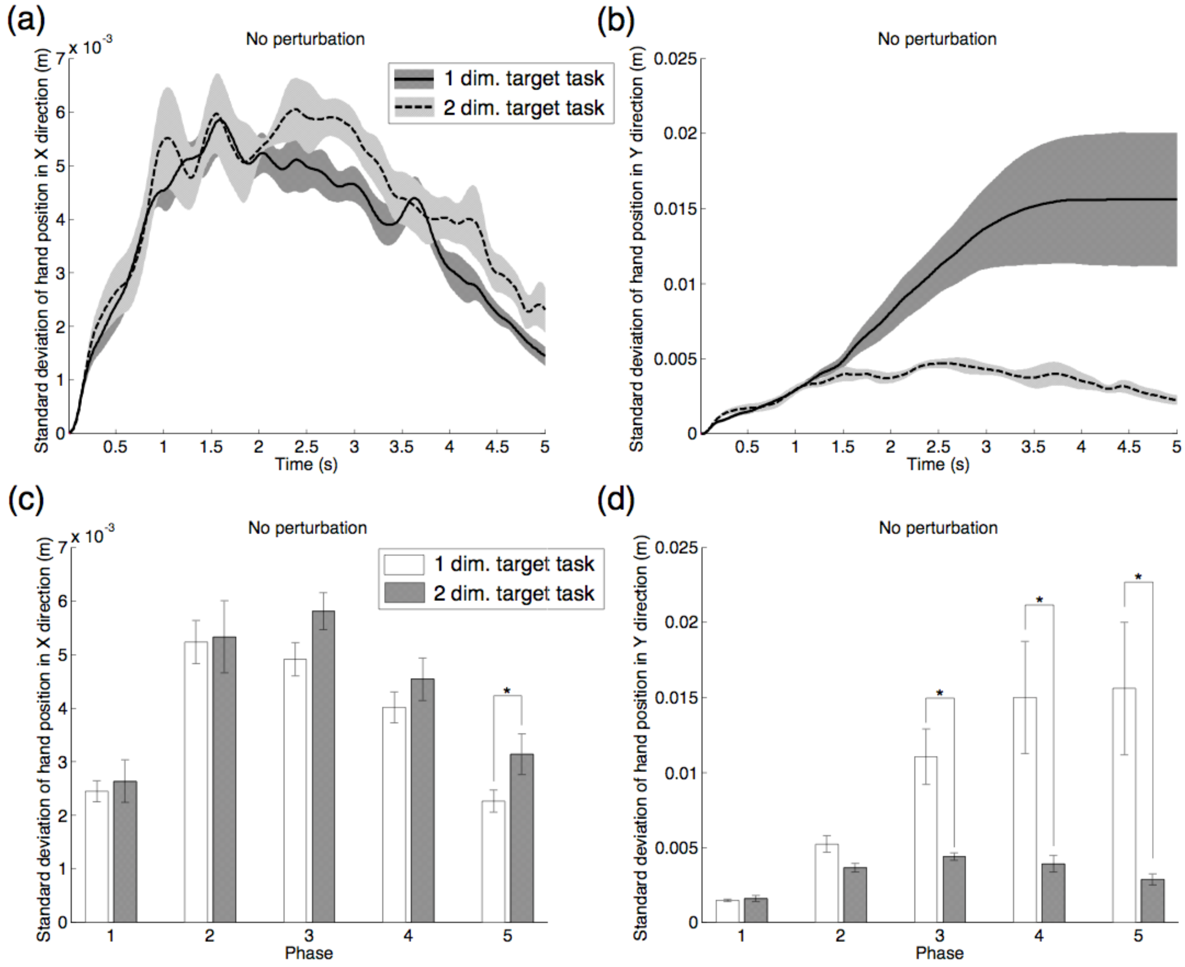

Fig. 3 The standard deviation of the hand position in the *X*-direction [(a) and (c)] and the *Y*-direction [(b) and (d)] of the trials without perturbation of all of the subjects. The upper figures indicate the time profile. The line and area denote the mean waveform and the standard error, respectively. The lower figures indicate the mean values in each phase (1 bin per 1 s). Asterisks denote significant differences between the standard deviation of the hand position in the one- and two-dimensional target-tracking tasks ($P < 0.05$).

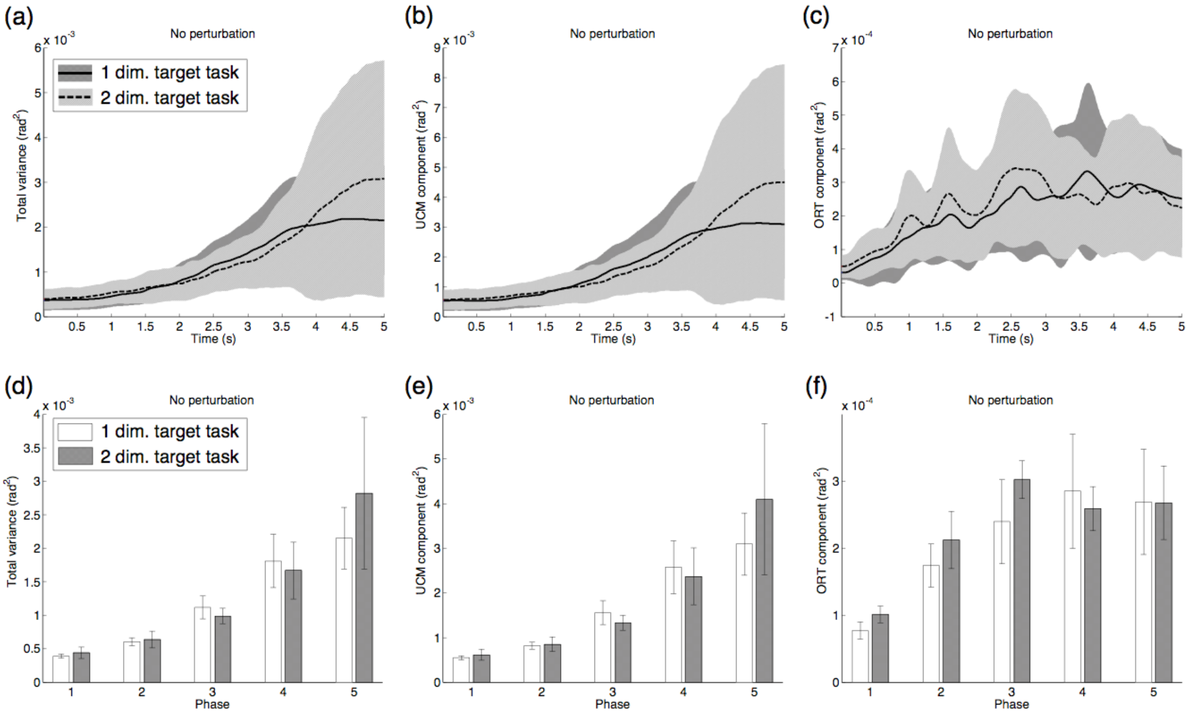

Fig. 4 The results of the UCM analyses for trajectories of unperturbed trials of all of the subjects. Left, center and right figures show the total variance [(a) and (d)], the UCM component [(b) and (e)] and the ORT component [(c) and (f)], respectively. The upper figures indicate the time profiles. The line and area denote the mean waveform and the standard error, respectively. The lower figures indicate the mean values in each phase (1 bin per 1 s).

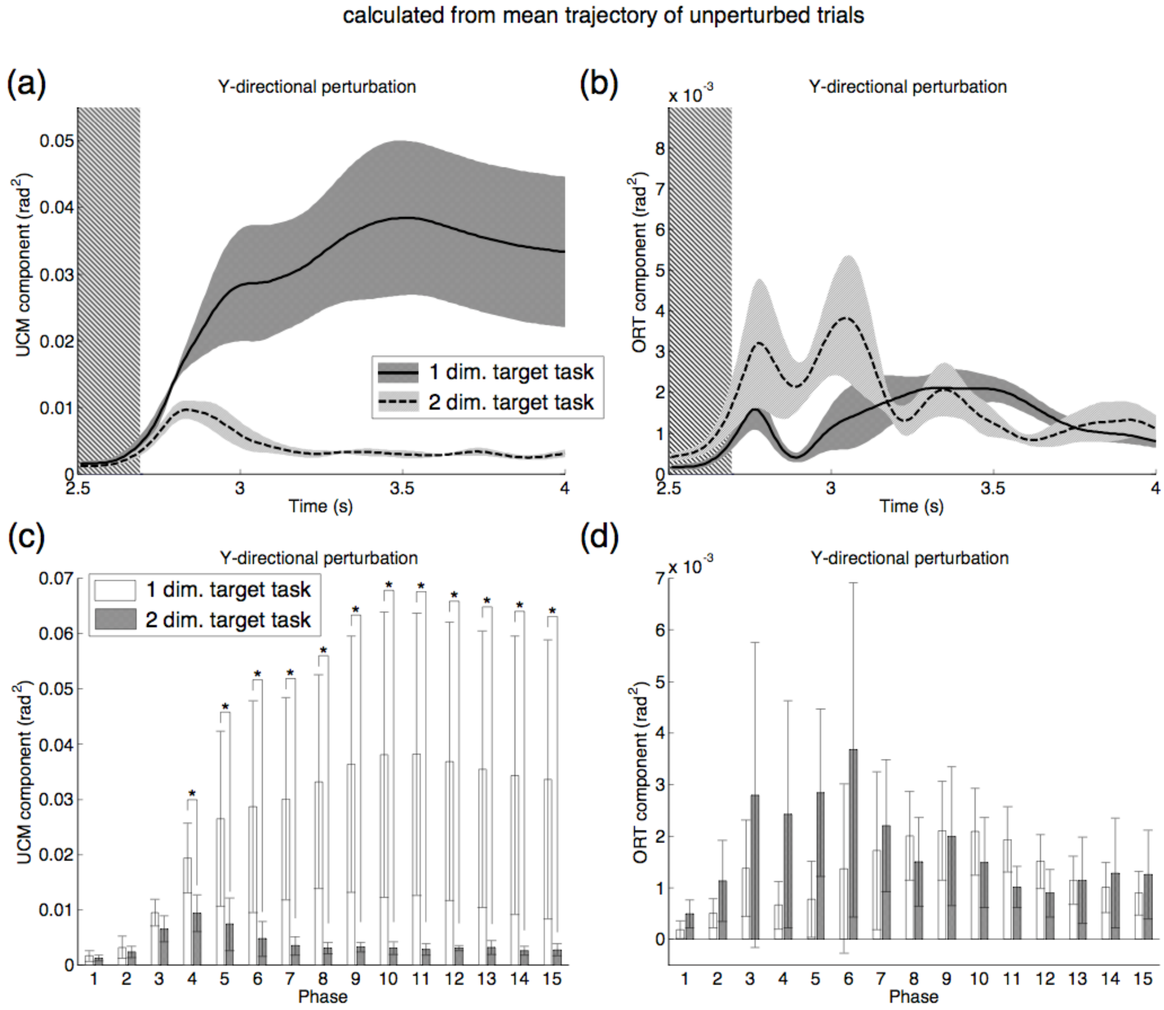

Fig. 5 The results of the UCM analyses of the trials with *Y*-directional perturbations of all of the subjects. (a) and (c) show the UCM component, and (b) and (d) show the ORT component. These component variances were calculated from the mean trajectories of the unperturbed trials. The upper figures indicate the time profiles. The gray rectangular area denotes the duration during which *Y*-directional perturbations were applied to the subjects' hands. The solid and dashed lines indicate the mean waveforms of the component variances in the one- and two-dimensional target-tracking tasks, respectively. The gray areas denote the range of the standard error in each task condition. The lower figures indicate the mean values in each phase (1 bin per 0.1 s). Asterisks indicate significant differences between the standard deviations of the hand positions in the one- and two-dimensional target-tracking tasks ($P < 0.05$).

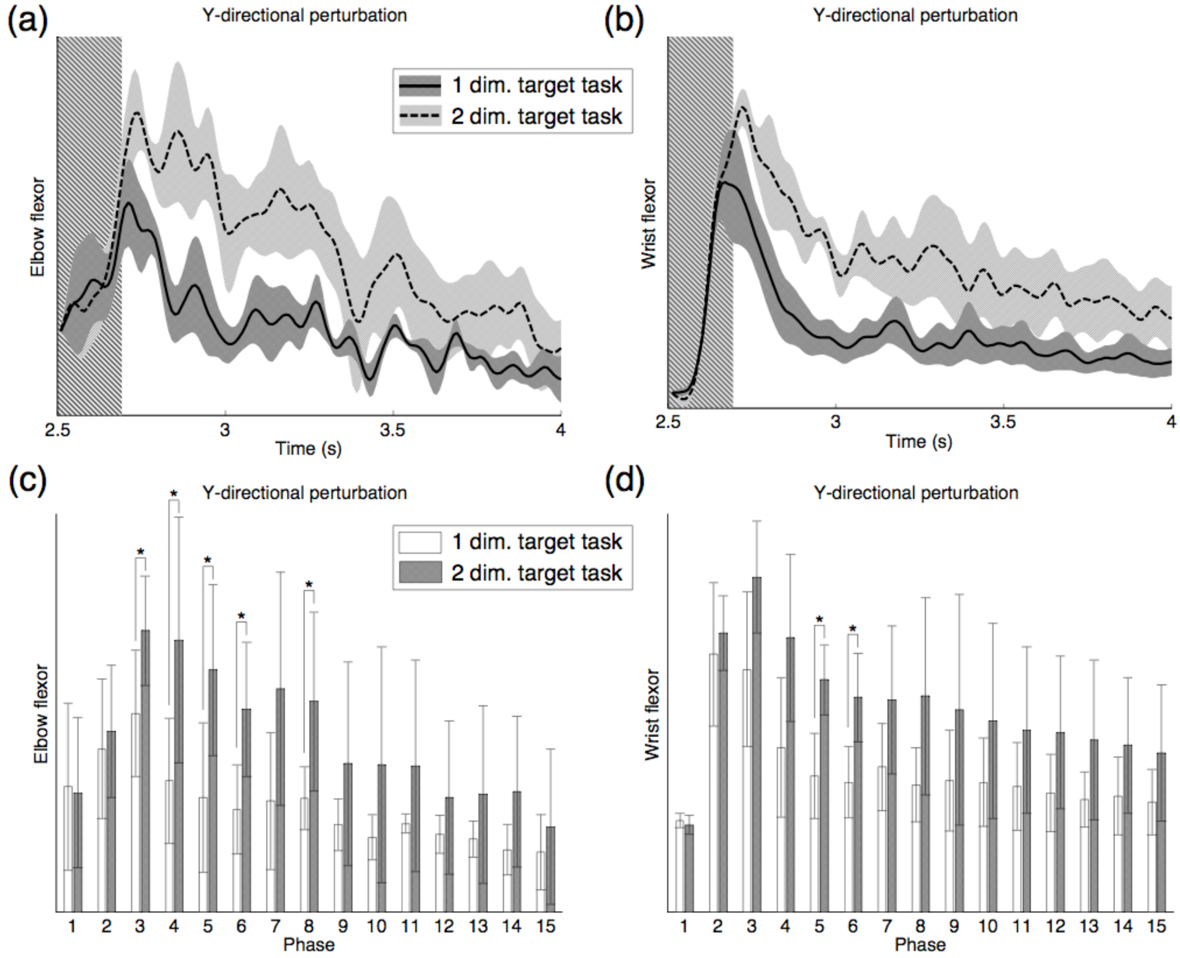

Fig. 6 The variations of the EMG signals of the biceps [(a) and (c)] and flexor carpi radialis [(b) and (d)] in trials with *Y*-directional perturbations of all of the subjects. The upper figures indicate the time profiles. The gray rectangular area denotes the duration during which anterior perturbations were applied to the subjects' hands. The solid and dashed lines indicate the mean waveforms of the EMG signals in one- and two-dimensional target-tracking tasks, respectively. The gray areas denote the ranges of the standard errors of the EMG signals in each task condition. The lower figures indicate the mean values in each phase (1 bin per 0.1 s). Asterisks indicate significant differences between the standard deviations of the hand positions in the one- and two-dimensional target-tracking tasks ($P < 0.05$).

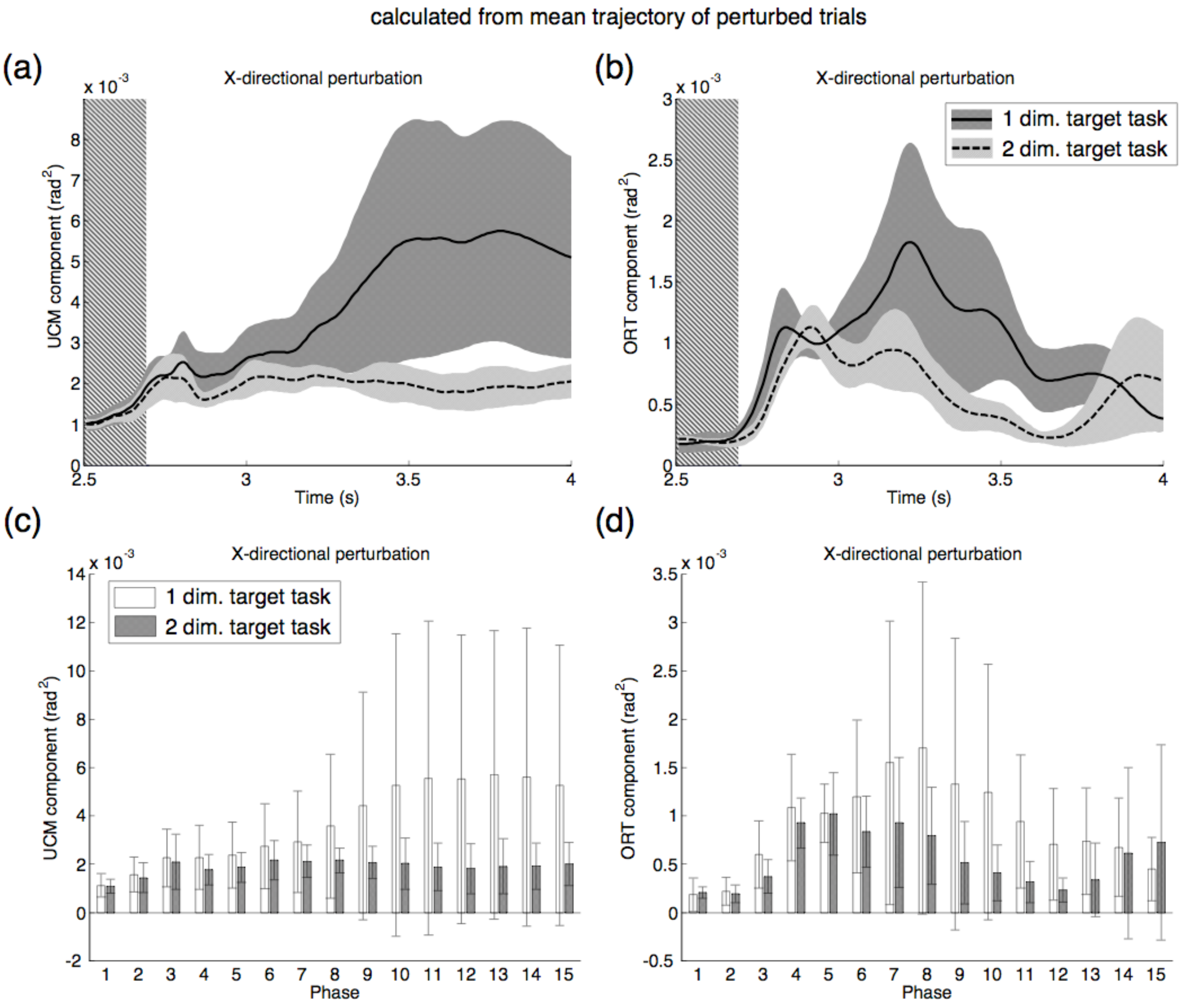

Fig. 7 The results of the UCM analyses of the trials with *X*-directional perturbations of all of the subjects. (a) and (c) show the UCM component, and (b) and (d) show the ORT component. These component variances were calculated from the mean trajectories of the X-directional perturbed trials. The upper figures indicate the time profiles. The gray rectangular area denotes the duration during which anterior perturbations was applied to the subjects' hands. The solid and dashed lines indicate the mean waveforms of the component variance in the one- and two-dimensional target-tracking tasks, respectively. The gray areas denote the range of the standard error of the component variance in each task condition. The lower figures indicate the mean values in each phase (1 bin per 0.1 s).

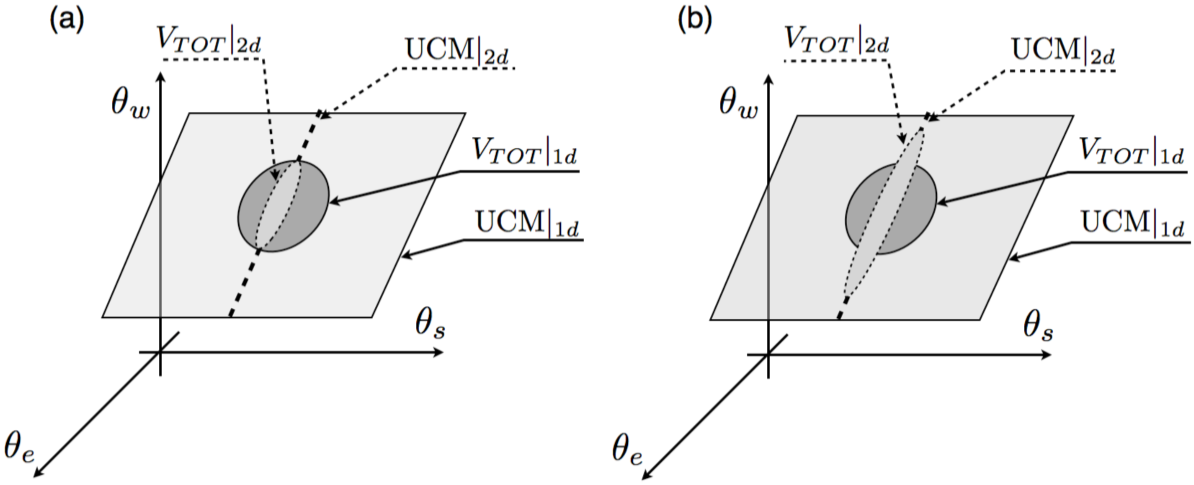

Fig. 8 Two types of strategy for constraints of task-irrelevant dimensions. The gray square area and black dashed line indicate UCM of one- and two-dimensional target-tracking task in joint space, respectively. Circle areas with solid and dashed lines denote total variance of one- and two-dimensional target tracking task, respectively. When the task-irrelevant dimension ($\mathrm{UCM}|_{1d}$) is constrained, (a) amount of total variance decreases ($V_{TOT}|_{1d} > V_{TOT}|_{2d}$) and variance along constrained task-irrelevant dimension ($\mathrm{UCM}|_{2d}$) remains, or (b) amount of total variance is unchanged ($V_{TOT}|_{1d} \cong V_{TOT}|_{2d}$) and variance along constrained task-irrelevant dimension ($\mathrm{UCM}|_{2d}$) increases. Applying same UCM analysis (using $\mathrm{UCM}|_{1d}$) in both tasks, the UCM component decreases (a) and is unchanged (b) in two-dimensional target-tracking task.